

Diffraction Line-Broadening Analysis of Al₂O₃/Y-TZP Ceramic Composites by Neutron Diffraction Measurement

K. Fan^{1,a}, J. Ruiz-Hervias^{2,b*}, C. Baudin^{3,c} and J. Gurauskis³

¹College of Materials Science and Engineering, Xihua University, Chengdu 610039, China

²Materials Science Department, Universidad Politécnica de Madrid, E.T.S.I. Caminos, Canales y Puertos, Profesor Aranguren 3, E-28040 Madrid, Spain

³Instituto de Cerámica y Vidrio, CSIC, Kelsen 5, E-28049 Madrid, Spain

^afankunyang123@126.com, ^bjesus.ruiz@upm.es, ^ccbaudin@icv.csic.es

Keywords: Ceramic Composites, Tape Casting, Neutron Diffraction, Peak Broadening, Microstrain

Abstract. Time-of-flight neutron diffraction was used for through-thickness measurement in a series of Al₂O₃/Y-TZP (alumina/tetragonal ZrO₂ stabilized with 3 mol.% Y₂O₃) ceramic composites. Different zirconia contents (5 vol.% and 40 vol.%) and green processing routes (a novel tape casting and conventional slip casting) were investigated. Diffraction line broadening analysis was carried out by using the Rietveld refinement method combined with the “double-Voigt” modelling to obtain the domain size and microstrain in the different phases. The results indicate that peak broadening is noticeable in zirconia (associated to microstrains) but not in alumina. The microstructure and non-uniform microstrains were mainly influenced by the Y-TZP content in the studied Al₂O₃/Y-TZP composites, irrespective of the measured direction and the fabrication process.

Introduction

Alumina-zirconia ceramics have received considerable attention in both engineering and academic fields due to their improved mechanical properties compared with pure alumina ceramics. Most of the previous research works [1] were focused on the uniform residual stresses between phases, without paying too much attention to the non-uniform microstrains at the grain and subgrain scales (type III stresses), maybe due to the tougher requirements both on the measurement and analysis procedures. Such non-uniform microstrains can reflect the existence of crystal defects (e.g., dislocations and crystal vacancies), which in turn will influence the mechanical properties of materials. Consequently, it is important to quantify the non-uniform microstrains of ceramics by using suitable measurement techniques and analysis methods.

Neutron diffraction is a preferred measurement technique to get information inside bulk samples, due to its high penetration depth. Based on the diffraction measurements, microstructural information of materials, e.g., crystal size and microstrain, can be extracted by diffraction line broadening analysis. Several approaches were established for quantification of line-broadening effects, e.g., the simplified integral-breadth methods, the Warren-Averbach procedure [2], and the traditional Williamson-Hall method [3]. Each method has its limitations and advantages, and sometimes conflicting results are obtained by different methods. Compared with other methods, the ‘double-Voigt’ approach [4] combined with Rietveld refinement shows its advantages in line broadening analysis for neutron data, especially in cases with limited *a priori* information, e.g., an arbitrary sample where significant peak overlap occurs.

In the present work, a series of Al₂O₃/Y-TZP (alumina/tetragonal ZrO₂ stabilized with 3 mol.% Y₂O₃) ceramic composites were studied. A novel tape casting route [5], which is better than



traditional casting methods both from the economic and environmental point of view, was used to fabricate the ceramic composites samples. Samples obtained with the conventional slip casting technique [6] were taken as reference for comparison. The time-of-flight (TOF) neutron diffraction technique was used for measurement in the studied ceramic composites. Line broadening analysis was carried out to obtain the microstructural information (domain size and crystal microstrain).

Materials and Methods

Materials. The studied $\text{Al}_2\text{O}_3/\text{Y-TZP}$ (3 mol.% Y_2O_3 stabilized zirconia) ceramic composites were prepared by two different green processing methods: the novel tape casting [5], and the conventional slip casting, as a reference technique. Two different contents of Y-TZP were used as reinforcement: 5 vol.% and 40 vol.%. The studied specimens were coded as A-5YTZP (slip), A-5YTZP (tape), A-40YTZP (slip), and A-40YTZP (tape), to describe their composition and fabrication technique.

High-density (relative density > 98 % theoretical density) materials were obtained after sintering for all the studied composites. The morphology of the chemical etched surface and the fracture surface of samples were observed by scanning electron microscopy (SEM, Zeiss DSM 950, Germany) and the average grain sizes of alumina and zirconia particles were determined.

Neutron Diffraction Measurements. For neutron diffraction strain scanning, sintered samples in the shape of parallelepipeds with dimensions $20 \times 20 \times 5 \text{ mm}^3$ were employed. Neutron diffraction data were collected on ENGIN-X time-of-flight instrument [7], at the ISIS, UK. The experimental setup consists of two detector banks which are centered on Bragg angles of $2\theta_B = \pm 90$ degrees. This setup allows simultaneous measurements in two directions of the sample: the in-plane (contained in the stacking plane) and the normal one (along the sample thickness). Through-thickness scanning was carried out along the sample thickness (approximately 5 mm), in 0.4 mm steps.

Data Analysis. The whole diffraction pattern was obtained in TOF diffraction measurements and then analyzed by Rietveld refinement, using the TOPAS-Academic V5 software package [8]. The diffraction profile is a convolution of instrumental and sample effects, where the latter is a combination of size and strain broadening. The overall quality of fitting was assessed in terms of R values [9], as obtained from the refinements.

In order to accurately determine the physical broadening, a correction of instrument broadening is essential. CeO_2 standard powder (cubic phase, space group $Fm\bar{3}m$, $a = 5.4114 \text{ \AA}$), as a highly crystalline sample which brings minimum sample broadening, was used as standard material for instrumental calibration. Good fits were achieved for the patterns of the CeO_2 standard powder recorded in each detector bank, with the weighed residual error R_{wp} ranging from 4 % to 8 %. The instrument-dependent parameters obtained from the fitting were fixed for subsequent refinement of the profiles corresponding to the ceramic composite samples.

After instrumental calibration, the sample effects, i.e., microstrain (strain broadening) and small crystallite size (size broadening), were analyzed by “double-Voigt” modelling. The crystallite size and microstrain values were determined [4], i.e., as volume-weighted domain size D_V and the average microstrain ϵ , respectively. Details of the refinement procedure are given in [10].

Results and Discussion

Microstructure. Very similar microstructures were found for the studied $\text{Al}_2\text{O}_3/\text{Y-TZP}$ samples with the same composition for both fabrication techniques, i.e. slip casting and tape casting. Fig. 1 shows the SEM micrograph of chemical etched surface and the fractured surface of the tape-cast $\text{Al}_2\text{O}_3/\text{Y-TZP}$ composites, as a function of zirconia content. X-ray diffraction analysis previously reported [11] that only $\alpha\text{-Al}_2\text{O}_3$ and tetragonal Y_2O_3 -stabilized zirconia (Y-TZP) phases were

found in the sintered ceramics. It can be seen that the alumina matrix (in dark grey) and zirconia particulates (in light grey) were generally well-dispersed in all the studied materials. Due to the inhibition effect of the second phase zirconia particles on matrix grain growth, the grain size of the Al_2O_3 matrix was decreased as the zirconia content increased from 5 vol.% to 40 vol.%, with the average value dropping from $1.9 \pm 0.3 \mu\text{m}$ to $1.1 \pm 0.2 \mu\text{m}$ (compare Fig. 1a with 1b). Narrow grain size distributions were observed for both phases in each composite.

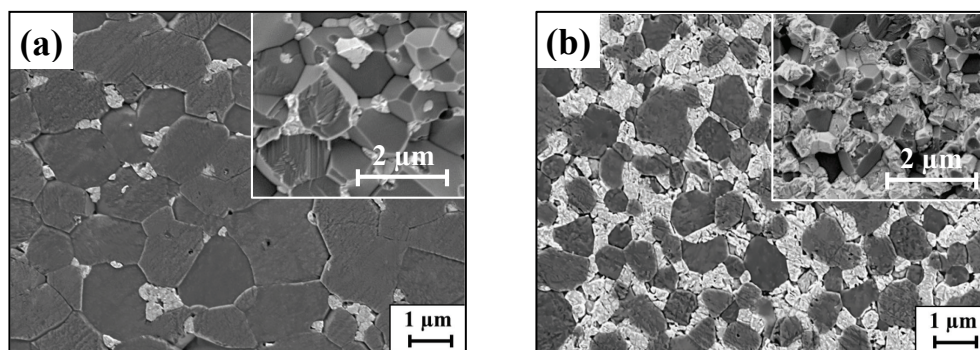


Fig. 1: SEM micrographs of chemical etched surfaces and fractured surface (the inset) of the studied tape casting materials: (a) A-5YTZP (tape) composites. (b) A-40YTZP (tape) composites. Al_2O_3 grains appear with dark grey color and Y-TZP particulates are in light grey color.

Peak broadening analysis. Diffraction profiles of samples were fitted without (only instrument broadening) and with sample physical broadening effect, respectively. As an example, the profile fitting of the A-40YTZP (tape) sample is presented in Fig. 2. The observed (measured) peak profile is shown as a blue line. The difference plot (difference between the observed and calculated intensities), is shown in grey below the spectra. The individual peaks of $\alpha\text{-Al}_2\text{O}_3$ and Y-TZP phases were identified with blue and black tick marks, respectively, below the profile. The strongest peaks of the Al_2O_3 (113) and Y-TZP (112) & (200) phases are shown in detail, in Figs. 2b and 2c, respectively.

If only the instrument effect is considered, as shown by the green line in Fig. 2, the sample contribution is not captured. The overall quality of fitting of the full profile with only instrument effect is far from optimum, with the weighted residual error R_{wp} ranging from 14~17 %, and the corresponding difference curves (in grey color below the spectra) showing remarkable fluctuations. The calculated peak profiles of Y-TZP reflections are narrower than the measured ones (Fig. 2c). However, such behavior is not noticeable in the Al_2O_3 reflections. With only instrument effect, the calculated Al_2O_3 peak profiles fitted the measured one quite well, as shown in Fig. 2b.

After introducing the sample physical contribution, i.e., crystallite size and microstrain, much better fitting (red line) was achieved, as can be judged from the flatter difference curves (black line below the spectra), as well as the lower $R_{wp} = 6 \%$. All of the Y-TZP and Al_2O_3 reflections were well fitted when the physical contribution to line broadening was taken into account.

Such peak broadening was observed in the Y-TZP reflections in all investigated samples, but it is almost negligible for the Al_2O_3 matrix. No obvious anisotropic broadening was observed in the profile fitting, which indicates the absence of texture or preferred orientation in the samples.

The “double-Voigt” modelling procedure for Al_2O_3 reflections gave unrealistic values of the size- and strain-related parameters, with very large error values. This indicates that there is no size or strain broadening in the Al_2O_3 phase, in agreement with the profile fitting behavior presented above. As a stable phase, negligible microstrains were reported for alumina in [12]. On the other hand, above a certain crystallite size ($\sim 1 \mu\text{m}$), size broadening is almost negligible in diffraction techniques. For the studied composites, the average grain size of the Al_2O_3 matrix was generally

larger than one micrometer (Fig. 1), and peak broadening was hardly observed.

For the Y-TZP phase, according to the analysis, peak broadening was mainly due to strain while

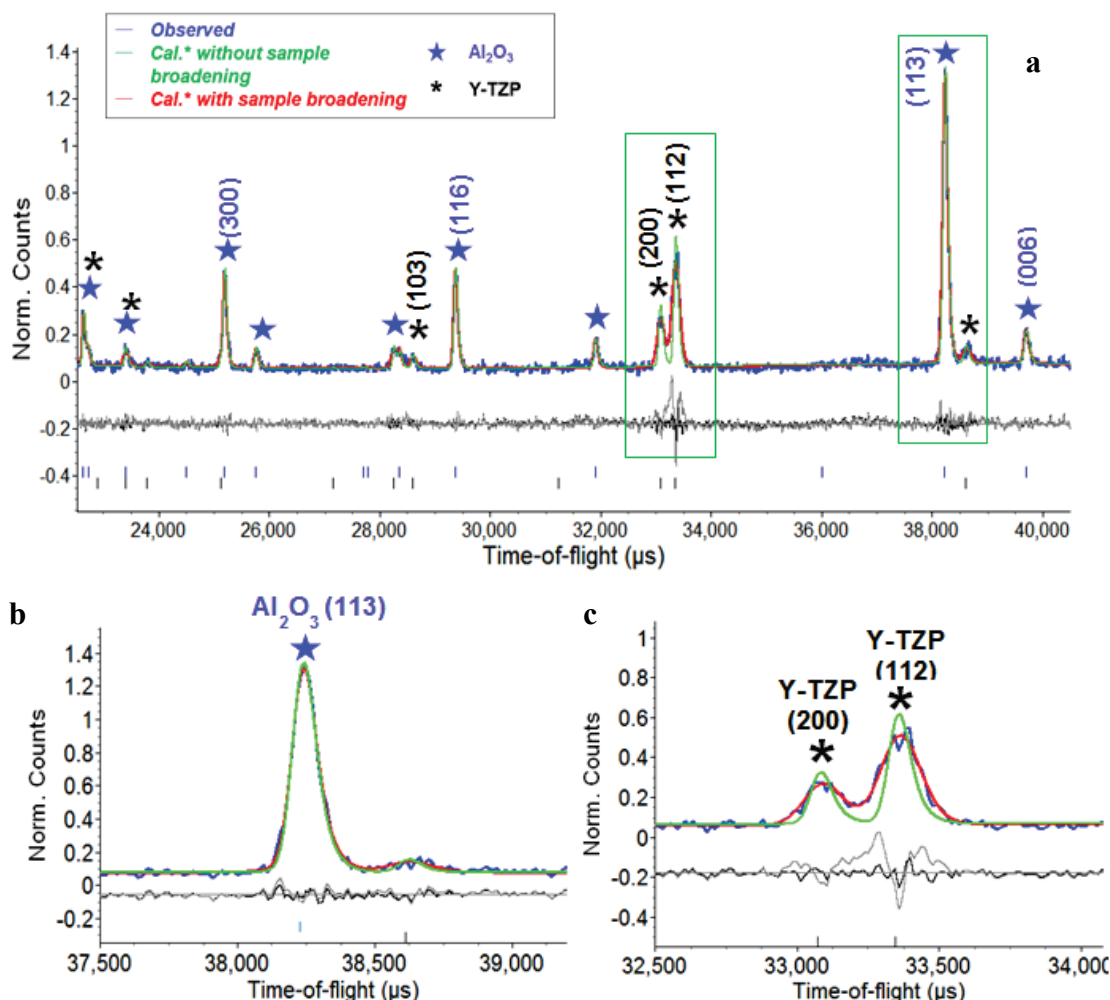


Fig. 2: Profile fitting for A-40YTZP (tape) sample: observed peak profile, blue line; fitting without physical broadening, green line, $R_{wp} = 15\%$; fitting with broadening, red line, $R_{wp} = 6\%$. (a) full profile; (b) Al_2O_3 (113) reflection; (c) Y-TZP (112) & (200) reflections.

size broadening effects were negligible. This might be explained by considering the zirconia phase transformation during fabrication. For the studied samples, 30 vol.% monoclinic ZrO_2 was found in the initial powders that was completely transformed to tetragonal phase during sintering [13]. It was reported [14] that atomic displacements occurred during the monoclinic to tetragonal zirconia phase transition in the alumina-zirconia system, mainly involving oxygen atoms. Some authors claim that a shearing mechanism also happens in the zirconia phase transformation [15]. In addition to that, an inhomogeneous distribution of yttria was observed during sintering in another work [12] with similar materials, which induces a defective core-shell structure of Y-TZP grains. All these factors could give rise to the observed microstrain in the Y-TZP.

The average microstrain (ϵ) values of Y-TZP are presented in Fig. 3. The data correspond to average values over different scanned positions in each sample, with standard errors represented by error bars. As the Y-TZP vol.% increases, a slight increase in microstrain ϵ in the Y-TZP crystallite was detected, changing from around $4 \cdot 10^{-4}$ in the A-5YTZP to $6 \cdot 10^{-4}$ in the A-40YTZP composites. This agrees with the findings of Wang *et al.* [16] and A. Reyes-Rojas *et al.* [17], which previously

reported a linear increase in microstrain with an increase in ZrO_2 % in the Al_2O_3 - ZrO_2 composites. The increase in microstrain in the Y-TZP crystallite would indicate that the number of lattice defects increases with the Y-TZP content. In addition, the obtained microstrain might provide an additional increment of local strain which would result in crack initiation and propagation.

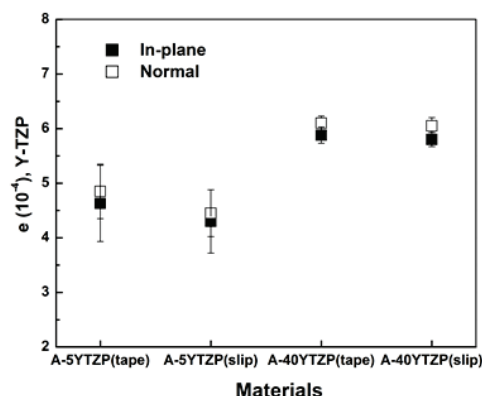


Fig. 3: The average microstrain, e , in Y-TZP in all of the studied Al_2O_3 /Y-TZP composites.

No significant difference was detected in the calculated microstrain of the Y-TZP due to the different manufacturing techniques employed in this work (tape casting and slip casting). The slight differences between the A-5YTZP (slip) and the A-5YTZP (tape) are included in the error bars, as shown in Fig. 3. Differences between the in-plane and the normal directions were also included within the experiment error bars for all composites samples.

Summary

A series of Al_2O_3 /Y-TZP bulk composites fabricated by different green processing (the novel tape casting and conventional slip casting) and with different Y-TZP content were investigated by time-of-flight neutron diffraction. Diffraction line broadening analysis was carried out by using the Rietveld refinement method to extract the microstructural information in the sample. Peak broadening in the Y-TZP reflections was observed in all investigated A/Y-TZP composites, but not in the Al_2O_3 reflections. The line-broadening of the Y-TZP peaks was mainly due to non-uniform microstrains. By increasing the Y-TZP content in the A/Y-TZP composites, the non-uniform microstrain e in the Y-TZP crystallite increased from around $4 \cdot 10^{-4}$ in the A-5YTZP to $6 \cdot 10^{-4}$ in the A-40YTZP composites. No obvious difference in microstructure and peak broadening was observed due to sample orientation (in-plane and normal directions) and the manufacturing processes (the novel tape casting and the conventional slip casting). Consequently, the quality of the ceramics manufactured using the novel tape casting method was proven (e.g., homogeneous microstructure, without undesired defects induced by the green processing method.). The quality of the ceramics manufactured using the novel tape casting method was proven (e.g., homogeneous microstructure, without undesired defects induced by the green processing method.).

References

- [1] M.E. Fitzpatrick, A.T. Fry, P. Holdway, F.A. Kandil, J. Shackleton and L. Suominen, Measurement Good Practice Guide No. 52 - Determination of Residual Stresses by X-ray Diffraction - Issue 2 (2005)
- [2] B. Warren and B. Averbach, The separation of cold work distortion and particle size broadening in X-ray patterns, J. Appl. Phys. 23 (1952) 497-497. <https://doi.org/10.1063/1.1702234>
- [3] G. Williamson and W. Hall, X-ray line broadening from filed aluminium and wolfram, Acta Metall. 1 (1953) 22-31. [https://doi.org/10.1016/0001-6160\(53\)90006-6](https://doi.org/10.1016/0001-6160(53)90006-6)

- [4] D. Balzar, N. Audebrand, M. Daymond, A. Fitch, A. Hewat, J. Langford, A. Le Bail, D. Louër, O. Masson and C. McCowan, Size-strain line-broadening analysis of the ceria round-robin sample, *J. Appl. Crystallogr.* 37 (2004) 911-924. <https://doi.org/10.1107/S0021889804022551>
- [5] J. Gurauskis, A. Sanchez-Herencia and C. Baudin, Joining green ceramic tapes made from water-based slurries by applying low pressures at ambient temperature, *J. Eur. Ceram. Soc.* 25 (2005) 3403-3411. <https://doi.org/10.1016/j.jeurceramsoc.2004.09.008>
- [6] A. Tsetsekou, C. Agrafiotis and A. Milias, Optimization of the rheological properties of alumina slurries for ceramic processing applications Part I: Slip-casting, *J. Eur. Ceram. Soc.* 21 (2001) 363-373. [https://doi.org/10.1016/S0955-2219\(00\)00185-0](https://doi.org/10.1016/S0955-2219(00)00185-0)
- [7] J. Santisteban, M. Daymond, J. James and L. Edwards, ENGIN-X: a third-generation neutron strain scanner, *J. Appl. Crystallogr.* 39 (2006) 812-825. <https://doi.org/10.1107/S0021889806042245>
- [8] A. Coelho, TOPAS-Academic V5, Coelho Software, Brisbane, Australia, <http://www.topas-academic.net/> (2012)
- [9] L. McCusker, R. Von Dreele, D. Cox, D. Louer and P. Scardi, Rietveld refinement guidelines, *J. Appl. Crystallogr.* 32 (1999) 36-50. <https://doi.org/10.1107/S0021889898009856>
- [10] K. Fan, J. Ruiz-Hervias, J.Y. Pastor, J. Gurauskis and C. Baudín, Residual stress and diffraction line-broadening analysis of Al₂O₃/Y-TZP ceramic composites by neutron diffraction measurement, *Int. J. Refract. Metals Hard Mater.* 64 (2017) 122-134. <https://doi.org/10.1016/j.ijrmhm.2017.01.011>
- [11] J. Gurauskis, Desarrollo de materiales laminados de alúmina-circona reforzados por tensiones residuales, (2006). Ph.D. dissertation (in Spanish)
- [12] C. Exare, J.M. Kiat, N. Guiblin, F. Porcher and V. Petricek, Structural evolution of ZTA composites during synthesis and processing, *J. Eur. Ceram. Soc.* 35 (2015) 1273-1283. <https://doi.org/10.1016/j.jeurceramsoc.2014.10.031>
- [13] K. Fan, J. Ruiz-Hervias, J. Gurauskis, A.J. Sanchez-Herencia and C. Baudín, Neutron diffraction residual stress analysis of Al₂O₃/Y-TZP ceramic composites, *Boletín de la Sociedad Española de Cerámica y Vidrio*, 55 (2016) 13-23. <https://doi.org/10.1016/j.bsecv.2015.10.006>
- [14] D. Simeone, G. Baldinozzi, D. Gosset, M. Dutheil, A. Bulou and T. Hansen, Monoclinic to tetragonal semireconstructive phase transition of zirconia, *Phys. Rev. B* 67 (2003). <https://doi.org/10.1103/PhysRevB.67.064111>
- [15] R. Patil and E. Subbarao, Monoclinic-tetragonal phase transition in zirconia: mechanism, pretransformation and coexistence, *Acta Crystallogr. A* 26 (1970) 535-542. <https://doi.org/10.1107/S0567739470001389>
- [16] X.L. Wang, C.R. Hubbard, K.B. Alexander, P.F. Becher, J.A. Fernandez-Baca and S. Spooner, Neutron diffraction measurements of the residual stresses in Al₂O₃-ZrO₂ (CeO₂) ceramic composites, *J. Am. Ceram. Soc.* 77 (1994) 1569-1575. <https://doi.org/10.1111/j.1151-2916.1994.tb09758.x>
- [17] A. Reyes-Rojas, H. Esparza-Ponce, S.D. De la Torre and E. Torres-Moye, Compressive strain-dependent bending strength property of Al₂O₃-ZrO₂ (1.5 mol% Y₂O₃) composites performance by HIP, *Mater. Chem. Phys.* 114 (2009) 756-762. <https://doi.org/10.1016/j.matchemphys.2008.10.044>